HERMETIC PACKAGES AND FEEDTHROUGHS FOR NEURAL PROSTHESES

Quarterly Progress Report # 1

(Contract NIH-NINCDS-N01-NS-4-2319)

(Contractor: The Regents of the University of Michigan)

For the Period:

October-December 1994

Submitted to the

Neural Prosthesis Program
National Institute of Neurological Disorders and Stroke
National Institutes of Health

By the

Center For Integrated Sensors and Circuits
Department of Electrical Engineering and Computer Science
University of Michigan
Ann Arbor, Michigan 48109-2122

Program Personnel:

Professor Khalil Najafi: Principal Investigator

Graduate Student Research Assistants:

Mr. Mark Nardin: Microstimulator Circuit Design/Fabrication

Mr. Jeffrey Von Arx: Electrode and Package Fabrication/Testing

Mr. Anthony Coghlan: RF Telemetry & Microstimulator Testing

Mr. Mehmet Dokmeci: Packaging and Accelerated Testing

February 1995

SUMMARY

The past quarter was the first quarter under our new contract aimed at the development of hermetic packages and feedthroughs for neural prostheses. Although the new contract has some specific new goals, the overall goal of developing long-term stable hermetic packages that we have pursued for the past few years is still central to the project. Therefore, we have continued the efforts that started under previous contracts and will focus on the specific goals of this contract as we proceed with it.

During the past quarter we achieved major progress in several areas, including the continued testing of our glass packages under accelerated conditions, the complete testing of the first generation microstimulator circuitry through an RF telemetry link, and preliminary testing of the second-generation microstimulator and its on-chip transmitter.

Our most significant results to date are those obtained from a series of silicon-glass packages that have been soaking in DI water at 85°C and 95°C for the past several months. We have four packages that have now lasted for more than 160 days at 85°C in DI water, and three packages that have lasted for more than 165 days at 95°C in DI water. We had originally started with 10 samples in each category. All those packages that did not survive were lost primarily due to handling or due to failure within the first day. These results are impressive in that they show for the first time that these packages can survive for a long time under accelerated conditions. We are now in the process of performing additional tests in saline solutions. We also have several packages soaking at room temperature in saline for over 60 days, and these have not shown any sign of leakage either.

We have just started implanting packages in rats to determine the biocompatibility and the integrity of the package materials in biological environments. No conclusive results have been obtained since the packages have not been explanted yet. Our plans aim at implanting more of these packages in both neural and muscular tissue in the next few months.

We have continued to improve our packaging techniques. A new glass fabrication technique based on ultrasonic micromachining of glass has been developed and used to fabricate capsules with much better surface quality. This new technique not only improves the bond surface planarity and roughness, it also reduces the fabrication cost and improves yield. We have ordered the first set of these packages which we should receive in the next few weeks. A new mask set for the fabrication of suitable silicon substrates for these packages has also been designed and sent out for fabrication. These substrates will be used to bond to the new glass capsules, and testing of the new structure will begin soon. We believe that the new structures will provide a much more uniform and much higher yield process.

During the past quarter we also finished the fabrication of the latest set of wafers containing both first- and second-generation microstimulators. The first-generation devices were tested both under probe station and using an RF telemetry link. Both tests were successful and we now have devices that are ready for complete assembly and use. During the next quarter we will assemble a number of these devices and will begin to encourage their use by external users. These first-generation devices provided the expected performance.

In addition to the first-generation devices we have started the testing of the second-generation devices. Preliminary results show that all the analog blocks of this system are functional. The digital blocks are not yet tested. An important part of the second generation device is the on-chip transmitter that utilizes an on-chip coil. This transmitter operates at 33MHz, draws about 1.2mA from a 5V supply and provides a range of several feet. This range is more than sufficient for our application. The transmitter coil is an on-chip electroplated Nickel coil which is integrated with the transmitter circuitry.

1. INTRODUCTION

This project deals with the development of hermetic, biocompatible micropackages and feedthroughs for use in a variety of implantable neural prostheses for sensory and motor handicapped individuals. The project also aims at continuing work on the development of a telemetrically powered and controlled neuromuscular microstimulator for functional electrical stimulation. The primary objectives of the project are: 1) the development and characterization of hermetic packages for miniature, silicon-based, implantable three-dimensional structures designed to interface with the nervous system for periods of up to 40 years; 2) the development of techniques for providing multiple sealed feedthroughs for the hermetic package; 3) the development of custom-designed packages and systems used in chronic stimulation or recording in the central or peripheral nervous systems in collaboration and cooperation with groups actively involved in developing such systems; and 4) establishing the functionality and biocompatibility of these custom-designed packages in *in-vivo* applications. Although the project is focused on the development of the packages and feedthroughs, it also aims at the development of inductively powered systems that can be used in many implantable recording/stimulation devices in general, and of multichannel microstimulators for functional neuromuscular stimulation in particular.

Our group here at the Center for Integrated Sensors and Circuits at the University of Michigan has been involved in the development of silicon-based multichannel recording and stimulating microprobes for use in the central and peripheral nervous systems. More specifically, during the past two contract periods dealing with the development of a single-channel inductively powered microstimulator, our research and development program has made considerable progress in a number of areas related to the above goals. A hermetic packaging technique based on electrostatic bonding of a custom-made glass capsule and a supporting silicon substrate has been developed and has been shown to be hermetic for a period of at least a few years in salt water environments. This technique allows the transfer of multiple interconnect leads between electronic circuitry and hybrid components located in the sealed interior of the capsule and electrodes located outside of the capsule. The glass capsule can be fabricated using a variety of materials and can be made to have arbitrary dimensions as small as 1.8mm in diameter. A multiple sealed feedthrough technology has been developed that allows the transfer of electrical signals through polysilicon conductor lines located on a silicon support substrate. Many feedthroughs can be fabricated in a small area. The packaging and feedthrough techniques utilize biocompatible materials and can be integrated with a variety of micromachined silicon structures.

The general requirements of the hermetic packages and feedthroughs to be developed under this project are summarized in Table 1. Under this project we will concentrate our efforts to satisfy these requirements and to achieve the goals outlined above. There are a variety of neural prostheses used in different applications, each having different requirements for the package, the feedthroughs, and the particular system application. The overall goal of the program is to develop a miniature hermetic package that can seal a variety of electronic components such as capacitors and coils, and integrated circuits and sensors (in particular electrodes) used in neural prostheses. Although the applications are different, it is possible to identify a number of common requirements in all of these applications in addition to those requirements listed in Table 1. The packaging and feedthrough technology should be capable of:

1- protecting non-planar electronic components such as capacitors and coils, which typically have large dimensions of about a few millimeters, without damaging them;
2- protecting circuit chips that are either integrated monolithically or attached in a hybrid fashion with the substrate that supports the sensors used in the implant;
3- interfacing with structures that contain either thin-film silicon microelectrodes or conventional microelectrodes that are attached to the structure;

Table 1: General Requirements for Miniature Hermetic Packages and Feedthroughs for Neural Prostheses Applications

Package Lifetime:

≥ 40 Years in Biological Environments @ 37°C

Packaging Temperature:

≤360°C

Package Volume:

10-100 cc

Package Material:

Biocompatible
Transparent to Light
Transparent to RF Signals

Package Technology:

Batch Manufactureable

Package Testability:

Capable of Remote Monitoring
In-Situ Sensors (Humidity & Others)

Feedthroughs:

At Least 12 with ≤125μm Pitch
Compatible with Integrated or Hybrid Microelectrodes
Sealed Against Leakage

Testing Protocols:

In-Vitro Under Accelerated Conditions
In-Vivo in Chronic Recording/Stimulation Applications

We have identified two general categories of packages that need to be developed for implantable neural prostheses. The first deals with those systems that contain large components like capacitors, coils, and perhaps hybrid integrated circuit chips. The second deals with those systems that contain only integrated circuit chips that are either integrated in the substrate or are attached in a hybrid fashion to the system.

Figure 1 shows our general proposed approach for the package required in the first category. This figure shows top and cross-sectional views of our proposed approach here. The package is a glass capsule that is electrostatically sealed to a support silicon substrate. Inside the glass capsule are housed all of the necessary components for the system. The electronic circuitry needed for any analog or digital circuit functions is either fabricated on a separate circuit chip that is hybrid mounted on the silicon substrate and electrically connected to the silicon substrate, or integrated monolithically in the support silicon substrate itself. The attachment of the hybrid IC chip to the silicon substrate can be performed using a number of different technologies such as simple wire bonding between pads located on each substrate, or using more sophisticated techniques such as flip-chip solder reflow or tab bonding. The larger capacitor or microcoil components are mounted on either the substrate or the IC chip using appropriate epoxies or solders. This completes the assembly of the electronic components of the system and it should be possible to test the system electronically at this point before the package is completed. After testing, the system is packaged by placing the glass capsule over the entire system and bonding it to the silicon substrate using an electrostatic sealing process. The cavity inside the glass package is now hermetically sealed against the outside environment. Feedthroughs to the outside world are provided using the grid-feedthrough technique discussed in previous reports. These feedthroughs transfer the electrical signals between the electronics inside the package and various elements outside of the package. If the package has to interface with conventional microelectrodes, these microelectrodes can be attached to bonding pads located outside of the package; the bond junctions will have to be protected from the external environment using various polymeric encapsulants. If the package has to interface with on-chip electrodes, it can do so by integrating the electrode on the silicon support substrate. Interconnection is simply achieved using on-chip polysilicon conductors that make the feedthroughs themselves. If the package has to interface with remotely located recording or stimulating electrodes that are attached to the package using a silicon ribbon cable, it can do so by integrating the cable and the electrodes again with the silicon support substrate that houses the package and the electronic components within it.

Figure 2 shows our proposed approach to package development for the second category of applications. In these applications, there are no large components such as capacitors and coils. The only component that needs to be hermetically protected is the electronic circuitry. This circuitry is either monolithically fabricated in the silicon substrate that supports the electrodes (similar to the active multichannel probes being developed by the Michigan group), or is hybrid attached to the silicon substrate that supports the electrodes (like the passive probes being developed by the Michigan group). In both of these cases the package is again another glass capsule that is electrostatically sealed to the silicon substrate. Notice that in this case, the glass package need not be a high profile capsule, but rather it need only have a cavity that is deep enough to allow for the silicon chip to reside within it. Note that although the silicon IC chip is originally 500μm thick, it can be thinned down to about 100μm, or can be recessed in a cavity created in the silicon substrate itself. In either case, the recess in the glass is less than 100μm deep (as opposed to several millimeters for the glass capsule). Such a glass package can be easily fabricated in a batch process from a larger glass wafer.

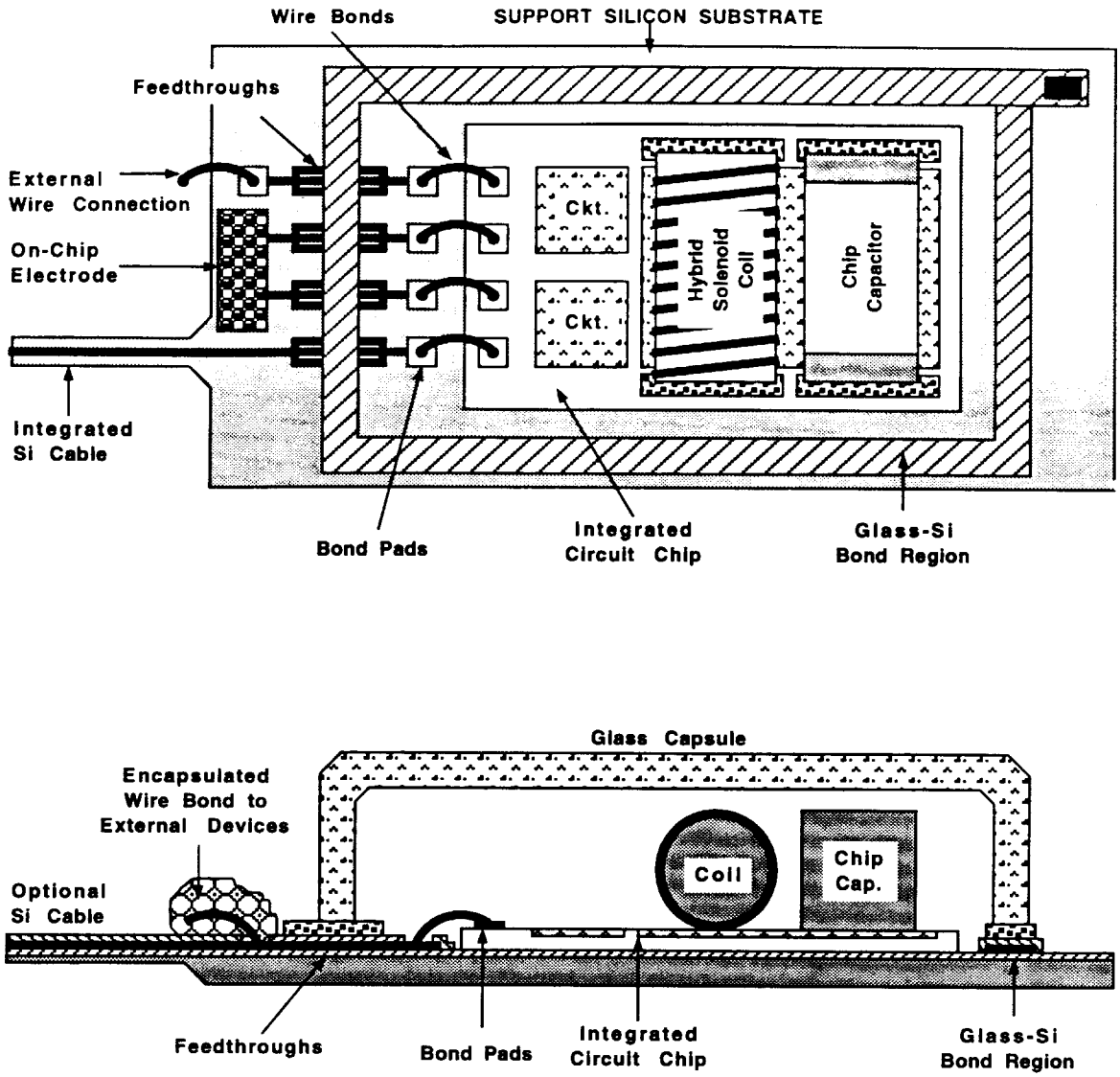

Figure 1: A generic approach for packaging implantable neural prostheses that contain a variety of components such as chip capacitors, microcoils, and integrated circuit chips. This packaging approach allows for connecting to a variety of electrodes.

We believe the above two approaches address the needs for most implantable neural prostheses. Note that both of these techniques utilize a silicon substrate as the supporting base, and are not directly applicable to structures that use other materials such as ceramics or metals. Although this may seem a limitation at first, we believe that the use of silicon is, in fact, an advantage because it provides several benefits. First, it is biocompatible and has been used extensively in biological applications. Second, there is a great deal of effort in the IC industry in the development of multi-chip modules (MCMs), and many of these efforts use silicon supports because of the ability to form high density interconnections on silicon using standard IC fabrication techniques. Third, many present and future implantable probes are based on silicon micromachining technology; the use of our proposed packaging technology is inherently compatible with most of these probes, which simplifies the overall structure and reduces its size.

Once the above packages are developed, we will test them in biological environments by designing packages for specific applications. One of these applications is in recording neural activity from cortex using silicon microprobes developed by the Michigan group under separate contracts. The other involves the chronic stimulation of muscular tissue using a multichannel microstimulator for the stimulation of the paralyzed larynx. This application has been developed at Vanderbilt University. Once the device is built, it will be used by our colleagues at Vanderbilt to perform both biocompatibility tests and functional tests to determine package integrity and suitability and device functionality for the reanimation of the paralyzed larynx. The details of this application will be discussed in future progress reports.

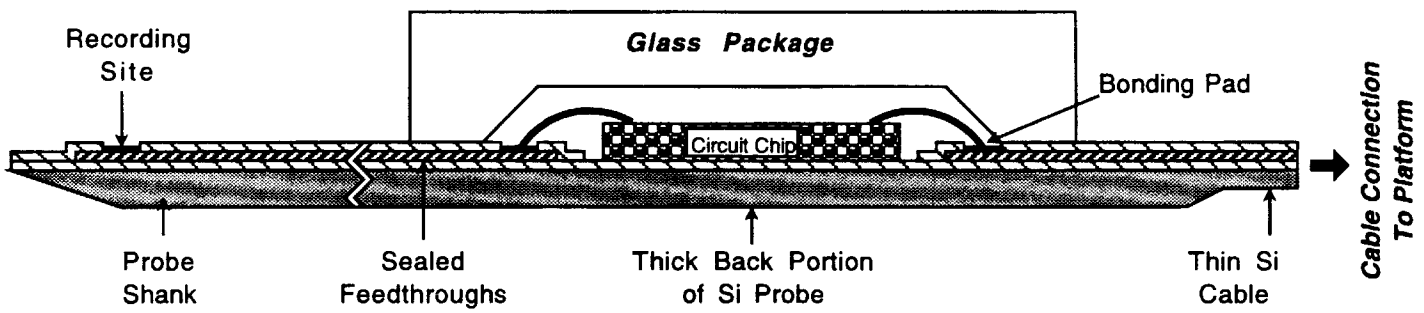

Figure 2: Proposed packaging approach for implantable neural prostheses that contain electronic circuitry, either monolithically fabricated in the probe substrate or hybrid attached to the silicon substrate containing microelectrodes.

2. ACTIVITIES DURING THE PAST QUARTER

2.1 Hermetic Packaging

Over the past few years we have developed a bio-compatible hermetic package with high density, multiple feedthroughs. This technology utilizes electrostatic bonding of a custom-made glass capsule to a silicon substrate to form a hermetically sealed cavity, as shown in Figure 3. Feedthrough lines are obtained by forming closely spaced polysilicon lines and planarizing them with LTO and PSG. The PSG is reflowed at 1100°C for 2 hours to form a planarized surface. A passivation layer of oxide/nitride/oxide is then deposited on top to prevent direct exposure of PSG to moisture. A layer of fine-grain polysilicon (surface roughness <40Å rms) is deposited and doped to act as the bonding surface. Finally, a glass capsule is bonded to this top polysilicon layer by applying a voltage of 2000V between the two for 10 minutes at 320 to 340° C, a temperature compatible with most hybrid components. The glass capsule can be either custom molded from Corning code #7740 glass, or can be batch fabricated using ultrasonic micromachining of #7740 glass wafers.

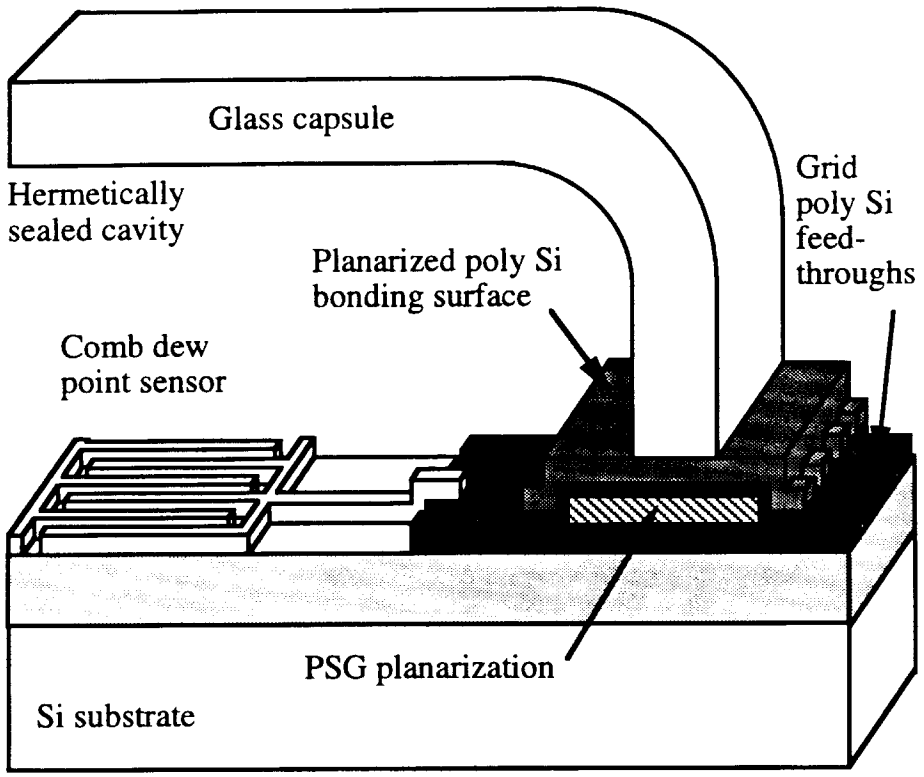

Figure 3: The structure of the hermetic package with grid feedthroughs.

During the past year we have electrostatically bonded and soak tested over 70 of these packages. We have found that we obtain the strongest and most reproducible bonds when we follow the bonding procedure outlined in Table 2. Subsequently, all of the packages used in the soak tests and the in vivo tests reported here have been bonded with this technique. We have found that with this technique we obtain a bonding yield of 80% (out of 30 capsules bonded with this technique, 5 failed within a day due to poor alignment of the glass capsule or surface defects), and with this technique our packages successfully prevent leakage in soak tests at 95° C for well over 2 months on average.

Table 2: Table outlining our bonding technique that consistently gives us high quality bonds.

Step	Comments
Packaging substrate is thinned	We have the best results when the package is thinned to between 100-150 μm (We believe that our new ultrasonically machined glass capsules will eliminate the need to thin the silicon wafer).
Capsule and substrate are solvent cleaned	Solvent clean consists of TCE, Acetone, IPA and finally DI water, all hot and with ultrasound agitation.
Conductive film is deposited on glass capsule	Either sputtered Aluminum or silver epoxy works well. We will use deposited metals with the new glass capsules.
Electrostatic bonding	Substrate is first placed on a 320 to 340°C hot plate and glass capsule is aligned. A Pyrex cover is then placed over the sample. Probes are lowered through a hole in Pyrex to make electrical contact. 2000V is applied for 10 minutes. Structure is cooled slowly (≈20 minutes to cool to RT).
Conductive coating removed	Aluminum etchant does this quickly.

2.1.1 Accelerated Soak Tests

We have continued our accelerated soak testing of our packages this quarter. For these tests we have chosen temperature as the acceleration factor because it is an easy variable to control, and because moisture diffusion is a strong (exponential) function of temperature. We started soaking 10 samples each at 95°C and 85°C in this series of tests. Tables 3 and 4 list some pertinent data for these soak tests. Figure 4 summarizes the results so far of our 95°C soak tests and Figure 5 summarizes the results so far of our 85°C tests. These figures also list the causes of failure for individual packages when it is known, and they show a curve fit to our lifetime data to illustrate the general trend. The curve fit, however, only approximates the actual package lifetimes since many of our packages failed due to breaking during testing rather than due to leakage.

All of these 85°C and 95°C soak tests have been performed in DI water. Originally we attempted to perform our high temperature soak tests in saline, but we found that in these tests the dominant failure mechanism was dissolution of the silicon substrate. We believe that this artificially shortens the measured lifetime of our packages because silicon does not appreciably dissolve in saline at body temperature, and we have started some tests to confirm this (to be discussed later in this report). In the mean time we have eliminated this failure mechanism by performing our accelerated soak tests in DI water. However, we do plan on beginning accelerated soak tests in saline again during the coming quarter.

Table 3: Key data for our 95°C soak tests.

Total number of packages in this study	**10**
Soaking Solution	**DI Water**
Number that failed prematurely (within 24 hours)	**1**
Longest lasting packages so far in this study (there are 2)	**164 Days**
Average lifetime assuming all remaining packages fail tomorrow (Worst case)	**77.3 Days**

Table 4: Key data for our 85°C soak tests.

Total number of packages in this study	**10**
Soaking Solution	**DI Water**
Number that failed prematurely (within 24 hours)	**2**
Longest lasting packages so far in this study	**159 Days**
Average lifetime assuming all remaining packages fail tomorrow (Worst case)	**84.8 Days**

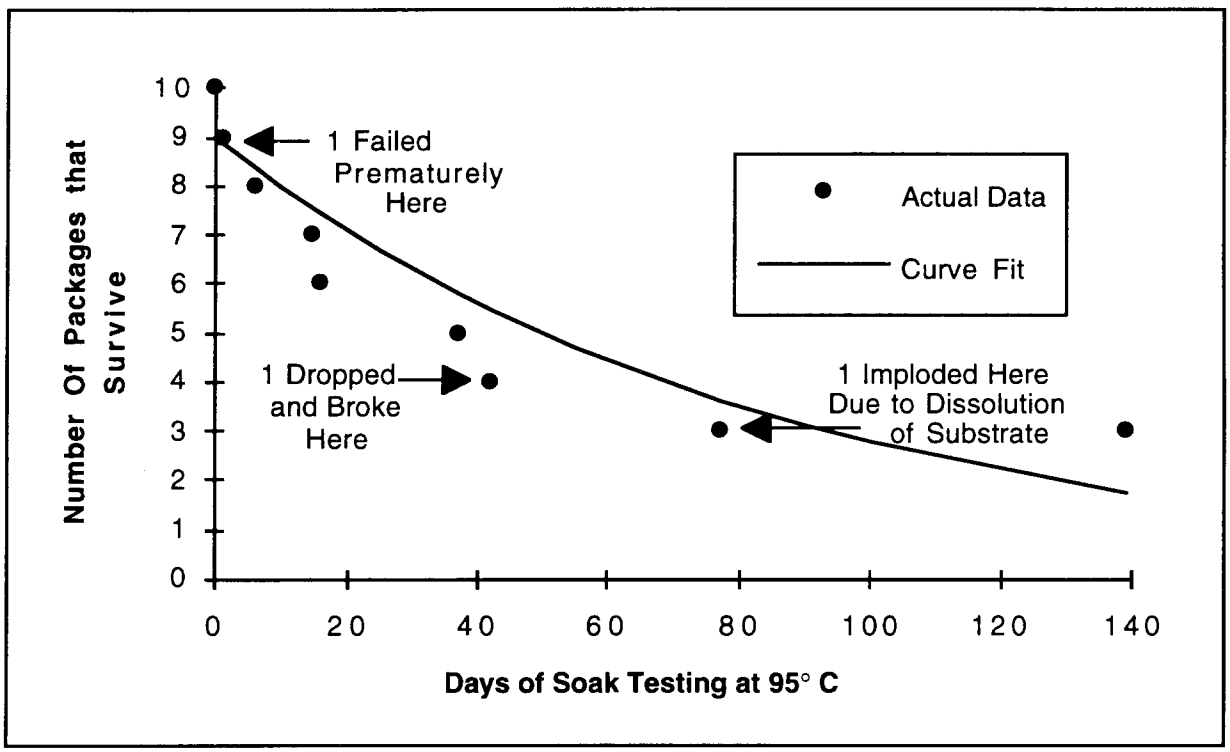

Figure 4: Summary of the lifetimes of our 10 packages which have been soak tested at 95°C this quarter.

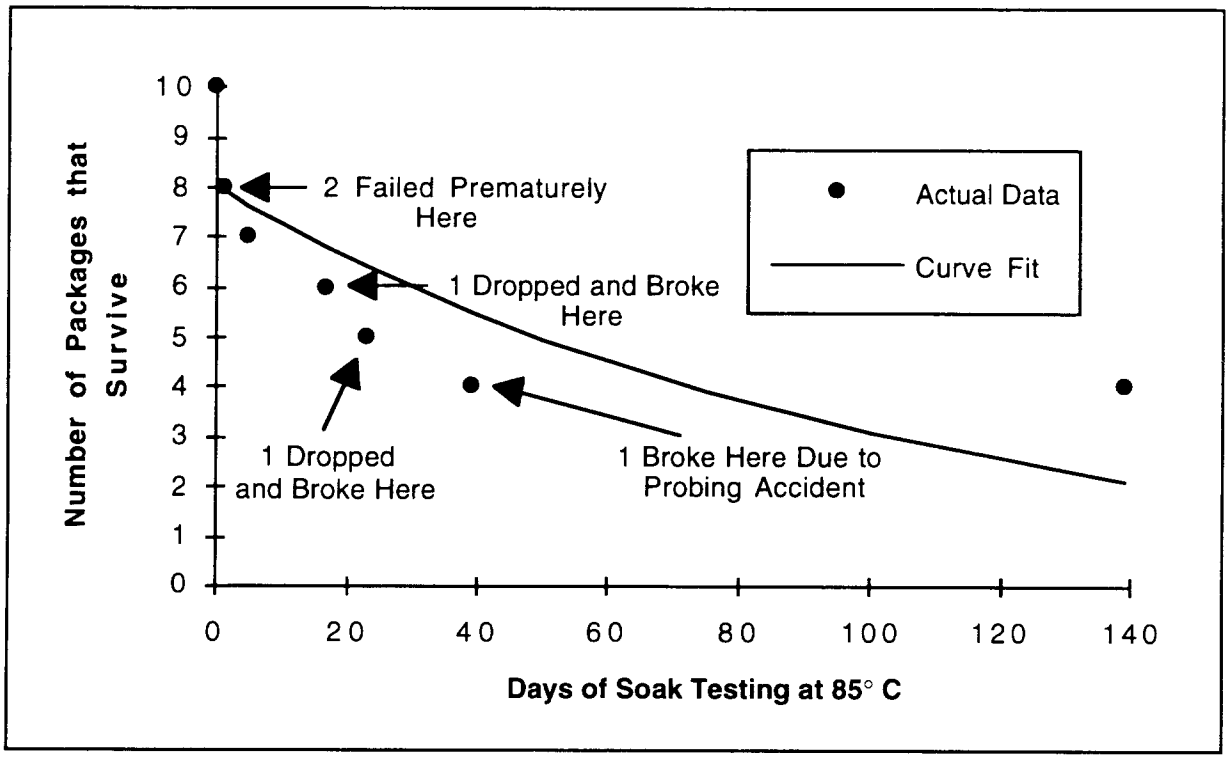

Figure 5: Summary of the lifetimes of our 10 packages which have been soak tested at 85°C this quarter.

All of these packages have been tested both electrically and visually. We define failure of the package to be when condensation occurs at room temperature (corresponding to ≈8% RH at 95° C and ≈11% RH at 85° C). The packages contain dew point sensors as shown in Figure 3, for electrically monitoring condensation. Figure 6 shows typical electrical measurements obtained from one of our dew point sensors as a function of package soaking time (soaking in DI water at 95°C) for a package that failed. As can be seen in the figure, we typically observe a 7° to 10° phase shift in the dew point sensor impedance when condensation occurs in our DI water soak tests. In contrast, dew point sensors on packages soaked in saline have a phase shift of 30° to 70° (depending on frequency) when saline penetrates the package. We also monitor for condensation visually. Condensation is easily seen on the inner surface of the glass capsule under a microscope. The photograph in Figure 7 compares two packages, one with condensation, and one without, to illustrate how easily condensation can be visually observed. In the particular package in Figure 6, condensation was measured after 17 days of soaking, and condensation was first observed visually after 21 days. Usually we can observe moisture a few days after we first measure it electrically. The fact that we have two independent methods for monitoring moisture inside of the packages provides additional confidence that our measured package lifetimes are correct.

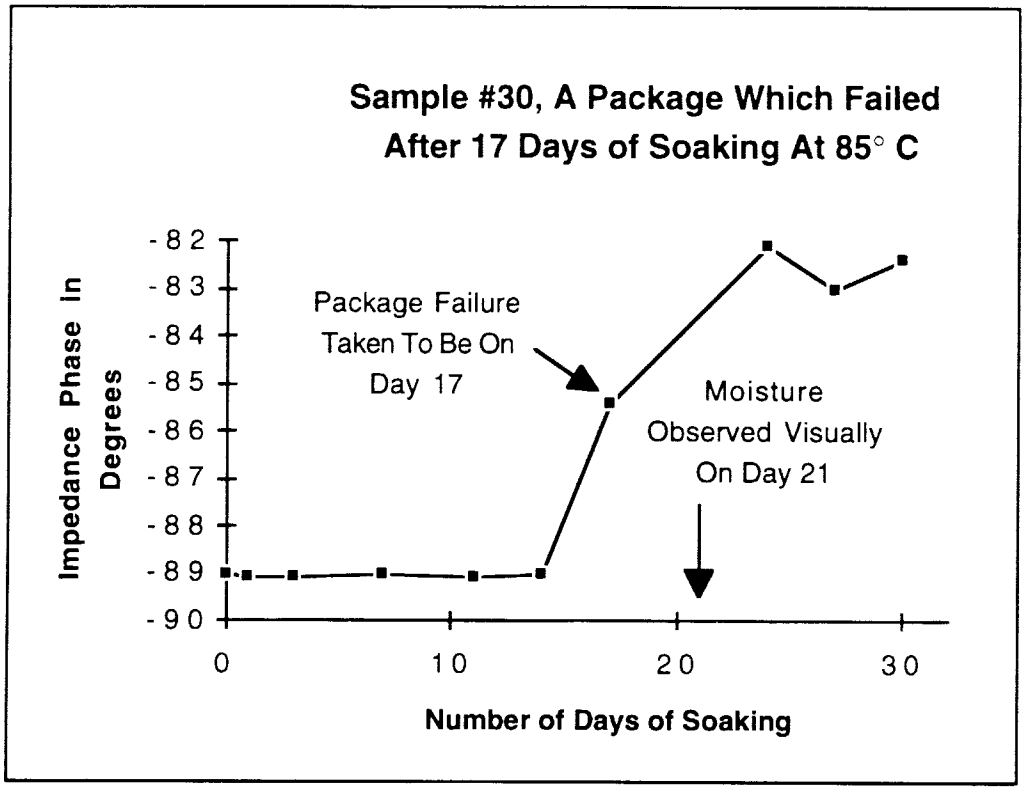

Figure 6: The impedance phase for a dew point sensor in a package soaking in DI water. This package failed after 17 days of soaking at 95°C.

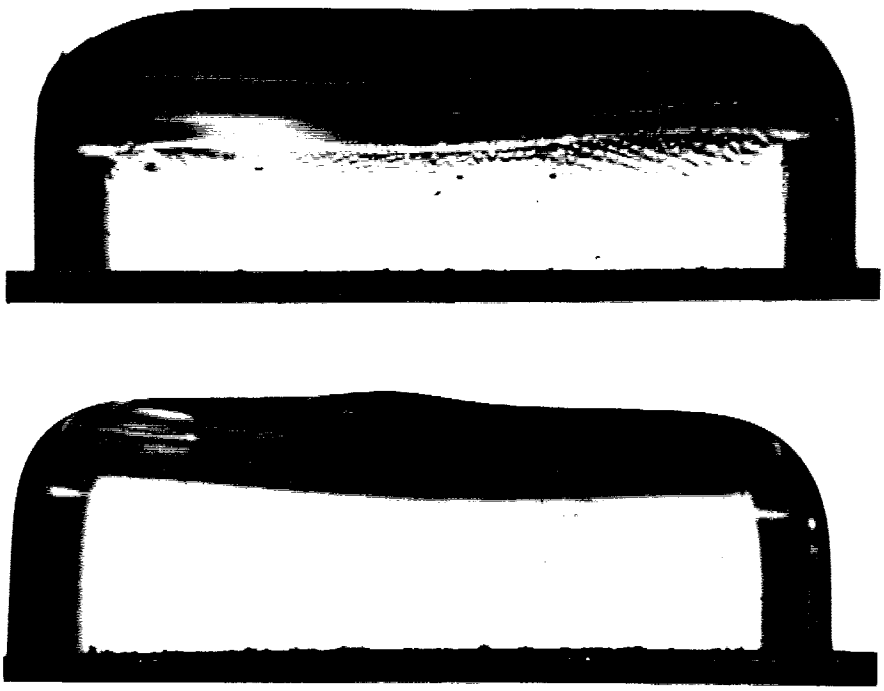

With Condensation

With No Condensation

Figure 7: A comparison of two packages; the top one has visible condensation after just 5 days of soaking at 95°C, while the bottom package has no condensation after 144 days soaking at 95°C.

The results obtained so far from our accelerated tests are very encouraging and indicate that indeed all of the modifications that we incorporated into the design of our package have been effective. We will continue our high temperature soak tests in the coming quarter. We plan on adding a number of new packages to these tests which we will soak in saline rather than DI water (we believe that we can stop the silicon dissolution problem we were having in our previous tests with an oxide/nitride/oxide coating on the back of the substrates, and through frequent changes of the saline solution). We also plan to fabricate our first true humidity sensors this coming quarter, and we will begin using these in our future tests. Finally, in the coming months we hope to begin using pressure as a second acceleration factor for our tests.

2.1.2 Dissolution of Silicon in Saline

We have observed silicon dissolution repeatedly in our high temperature soak tests in saline. In the worst cases, almost half of our ≈100 μm thick silicon substrate has dissolved away after just soaking for a few weeks. This is the reason that up until now all of our long term soak tests have been performed in DI water. We have found that silicon dissolution occurs much more slowly in DI water than in saline at high temperatures. It is important to note that we have not observed dissolution of silicon in saline at body temperature or room temperature.

As soon as we noticed dissolution of our substrates in our high temperature soak tests, we examined some packages from our long term soak tests under the SEM to measure the remaining substrate thickness. The results of these measurements are summarized in Table 5. From the remaining substrate thicknesses, approximate dissolution rates were calculated. The average dissolution rates for these samples are: 1.8 μm/day at 95° C and 0.7 μm/day at 85° C.

Table 5: Measured silicon dissolution rate in our long term soak tests.

Days of Soaking	Soak Test Temp.	Soaking Solution	Substrate Thickness (from SEM)	Comments
32	95° C	1 week in saline, then DI Water	85 μm	This sample had virtually no damage
77	95° C	1 week in saline, then DI Water	33 μm	So much of the substrate etched away that the sample finally imploded
39	85° C	DI Water Only	125 μm	This sample had virtually no damage
1	85° C	DI Water Only	153 μm	This sample was our control sample, because it was only soaked for 1 day

After observing this dissolution of silicon, we performed some tests to begin characterizing it. We examined the temperature dependency of the dissolution by soaking some substrates at two different temperatures (85°C and 95°C) and examining them after 1 week for substrate thinning and surface pitting. We examined the dependency on soaking solution by soaking some in saline and some in DI water for 1 week and again examining for thinning and pitting. Finally we soaked some of our actual packaging substrates as well as some bare silicon substrates to ascertain whether or not the dissolution process was unique to our structure as some electro-chemical processes might be. A summary of our observations for bare silicon substrates under all of our different soaking conditions is given in Table 6, and a summary of our observation for our actual package substrate is given in Table 7. The results of these tests indicate that the dissolution rate is a strong function of temperature, a strong function of the soaking solution, and it is not unique to our structure, nor does it appear to be faster in our structure than in bare silicon.

Table 6: Summary of the results of dissolution experiments on bare silicon.

Substrate	Soaking Solution	Temp	Observations After 1 week of Soaking
Bare Silicon (500μm thick)	DI Water	85° C	No appreciable etching
Bare Silicon (500μm thick)	Saline	85° C	Etching just started (some inverted pyramids). Etching is particularly bad at one corner
Bare Silicon (500μm thick)	DI Water	95° C	Definite etching. Wafer surface very rough, although no inverted pyramids.
Bare Silicon (500μm thick)	Saline	95° C	Inverted Pyramids obvious from front side. Etching is particularly bad along one entire edge

Table 7: Summary of the results of dissolution experiments on packaging substrate.

Substrate	Soaking Solution	Temp	Observations After 1 Week of Soaking
Package Substrate (≈100μm thick)	DI Water	85° C	Aluminum etched completely away. No other layers had any signs of etching.
Package Substrate (≈100μm thick)	Saline	85° C	Aluminum etched completely away. Polysilicon bonding region completely etched away.
Package Substrate (≈100μm thick)	DI Water	95° C	Aluminum etched completely away. Poly bonding region completely etched away.
Package Substrate (≈100μm thick)	Saline	95° C	Substrate thinned by at least 50μm. Aluminum etched completely away. Poly bonding region completely etched away. Etch pits everywhere (round pits).

It is our belief that dissolution of silicon is not significant at body temperature. Neural probes and ribbon cables have been implanted for years without observing any dissolution. It is however something to watch out for in our accelerated tests. It is a dominant failure mechanism for our high temperature accelerated soak tests in saline, and has forced us to temporarily perform our high temperature soak tests in DI water. However we would like to test our packages in as close a solution to biological fluids as we can. We plan on beginning some high temperature soak tests in saline in the coming quarter. For these devices we will leave a thermally grown silicon dioxide coating on the back of the substrate to protect it from dissolution. It should be noted that oxide/nitride/oxide is on the back side of our wafers when we finish fabrication and we go out of our way to remove it before thinning the substrates for electro-static bonding. We believe that with our new ultrasonically machined glass capsules, we will not have to thin the substrate before bonding because the capsule should be much more planar than the molded capsules which we have been using. Because we should not have to thin the substrates before bonding, we do not have to remove the dielectrics from the back side. These dielectrics should stop dissolution from occurring. The front side of our package substrates have dielectrics and we have seen very little dissolution on the front side. Should dissolution continue to be a problem and we find that dielectrics do not slow it enough, we will explore other techniques and other films to slow/stop this dissolution altogether.

2.1.3 Room Temperature Soak Tests

We began some long term soak tests in phosphate buffered saline at room temperature this past quarter. We started these tests for two reasons. First, we want to obatin test results in saline, and so far we have only been able to perform accelerated tests in DI water due to the dissociation of silicon in saline at high temperature. Secondly, we want some soak test data independent of the acceleration technique used. Admittedly, the room temperature tests will take a long time to produce any meaningful data. However, the results obtained this way will act as a good control technique to verify the overall integrity of our package. It should be noted that we are also setting up to perform some tests at 37°C to more closely mimic the body environment.

We soaked 6 packages in saline at room temperature this past quarter. Two of these packages leaked within a day, indicating surface defects or poor bonding during alignment. The remaining 4 packages are all still soaking with no sign of moisture either measured electrically or observed visually. Three of these four packages have been soaking now for 61 days, and the one remaining package has been soaking for 28 days.

We plan on continuing our room temperature soak tests indefinitely, and increase the number of samples in this test during the coming quarter. We will continue to update our results in future progress reports.

2.1.4 In-Vivo Tests

We began preliminary in-vivo testing of our hermetic packages this quarter. Three devices have been implanted in two guinea pigs at Kresge Hearing Research Institute. The first animal was implanted with two devices on January 17, 1995, and the second animal was implanted with one package on February 2, 1995. We plan on leaving the devices in for 2 months. All of these devices have been implanted on the dura. Part of the skull was removed so that the packages sit between the dura and the skin. This placement is compatible with the eventual placement of the hermetically-sealed telemetry platforms for application in the CNS.

We have defined four goals for these initial in-vivo tests. First of all, we hope to test the mechanical strength and durability of the package in an in-vivo environment. Secondly, we hope to obtain some hermeticity/leakage data on the packages in an in-situ environment. We will obtain this data by testing the packages for leakage after they are removed from the animals, provided of course that the packages do not break. Third, we hope to obtain bio-compatibility data on the geometric shape and of the materials used in our package. Finally we hope to examine the package substrate and surface films for any dissolution. We do not expect to observe any dissolution at all at body temperature, but it is important to confirm this in-situ.

In the coming quarter we hope to begin our in-vivo studies in muscular tissue at Vanderbilt University, as well as continue our dura testing at KHRI. Our next quarter report will detail the results of these initial in-vivo studies, and will discuss the protocols for those tests to be performed at Vanderbilt.

2.1.5 Improved Packaging Design

The glass capsules that we have been using up until now have worked well in our hermeticity testing, but they do have some problems. First, the individually molded glass capsules are expensive (about $20 each). Secondly the specification to which the surface can be polished is limited due to the small and awkward shape of the molded capsule. Third, we have found that the bonding surface is not as planar and flat as we require. To overcome this we have

had to thin the silicon substrate down to 100μm so that they are more conformal to curvature in the glass. As we have reported previously, ultrasonically machined glass capsules should overcome all of these problems. Ultrasonically machined glass capsules are much less expensive (about $3 each), and can be polished to a much better flatness and smoothness because polishing is done at the wafer level with standard wafer polishing techniques. For review, the Ultrasonic machining process is illustrated in Figure 8.

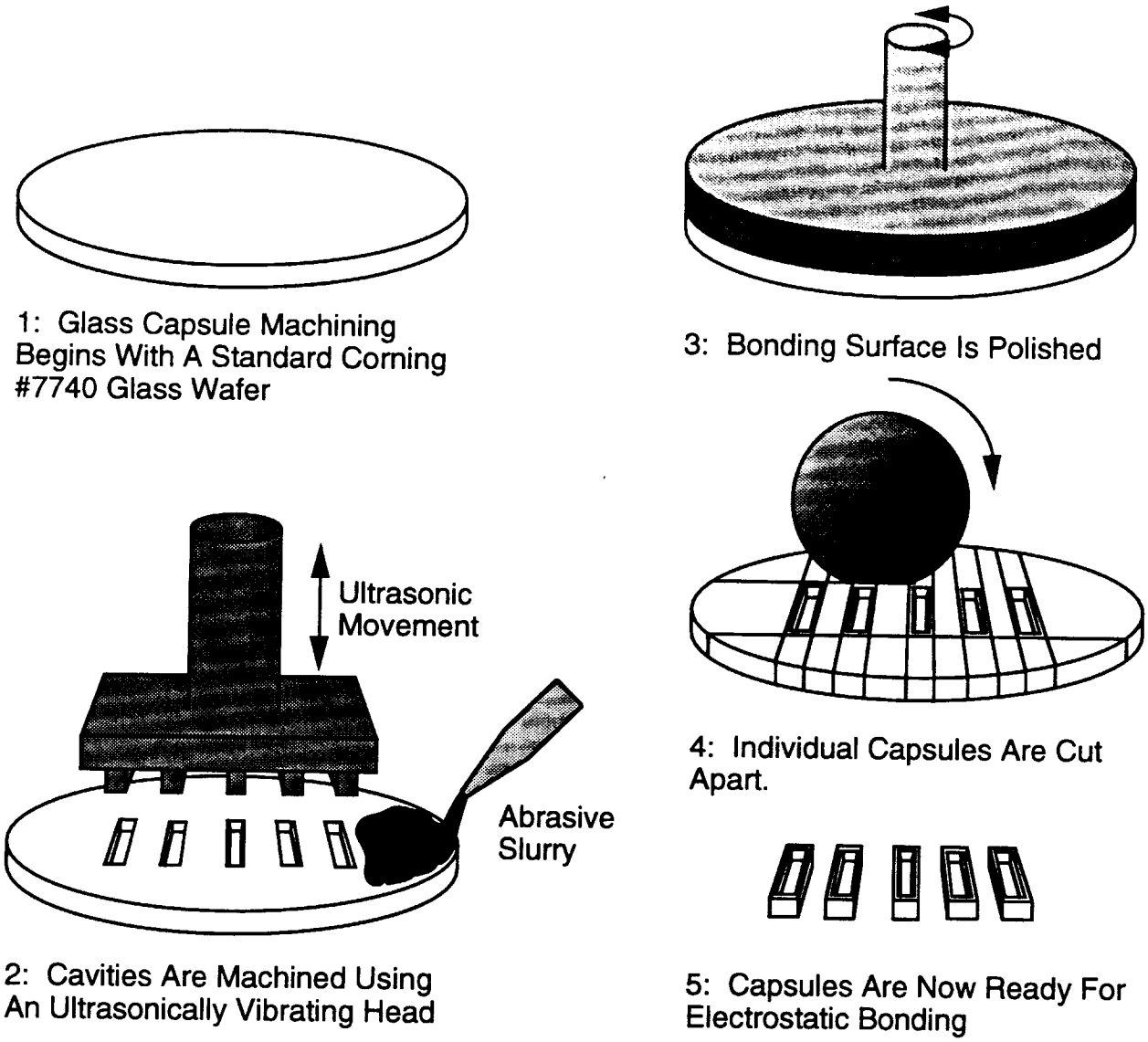

Figure 8: The fabrication process for ultrasonically machined glass capsules.

This quarter we ordered our first batch of ultrasonically machined glass capsules, and they are due to be shipped to us in mid-February. We have ordered 500 each of two different size glass capsules. One has interior dimensions of 9.2mm X 1.8mm X 2.0mm and is designed to fit the single channel microstimulator circuitry, while the second has interior dimensions of 15.0mm X 1.8mm X 2.0mm and is designed to fit the multi-channel microstimulator circuitry. The single channel microstimulator glass capsule is slightly larger than the molded glass capsules that we have been using in our soak tests and our in-vivo tests. This is because the circuitry is slightly larger than originally anticipated. Primarily because of this size difference and because the ultrasonically machined glass capsules have square corners rather than the rounded corners of the molded glass capsules, an entirely new mask layout was done this quarter to match the new glass capsules.

The new layout contains a package for the single-channel microstimulator, a package for the multi-channel microstimulator, and two test packages containing both buffered and un-buffered dew point sensors. The test packages also contain our first humidity sensor, which is a parallel plate capacitive device that uses polyimide as a moisture sensitive dielectric. Another notable change in our test package design is that we now have four leads going to every dew point and humidity sensor rather than just two. Having four leads gives us two advantages. First it gives us a continuity check to make sure that our leads are not open, and secondly it allows us to negate contact resistance and lead resistance by 4-point probing.

We should have our mask set for our new package layout back within a week, and fabrication will begin right after that. Our next progress report will contain some preliminary test results from our new packages. Also during the coming quarter we plan on laying out, fabricating and beginning tests on a low profile package which will be more conducive to in-vivo tests. The low profile package will be designed to package circuitry with no discrete components such as the microstimulator's coil and capacitor. This low profile package layout will also include integrated ribbon cables to allow in-situ monitoring of humidity sensors in our in-vivo implanted packages.

2.2 Implantable Microstimulators

2.2.1 Single-Channel Microstimulator

Figure 9 shows the circuit block diagram for the single-channel microstimulator. Over the past quarter we finished fabrication of this circuitry, and Figure 10 shows a picture of the latest fabricated circuit for the first generation microstimulator. The fabrication process was delayed by 6 weeks due to equipment down-time in our laboratory. Presently, we have two completely finished wafers that we have been testing. There are four other wafers ready for the final metallization step, five wafers ready for the second polysilicon step, and six wafers ready for gate oxidation and the first polysilicon layer. We have left these wafers behind at these points in case there were any processing problems. We have begun testing the finished circuitry and have been able to demonstrate a fully functional microstimulator both on a probe station and with a wireless telemetric link. The following will describe our results from telemetrically powering and operating the device and of the operation of various circuit blocks.

This past quarter we tested the latest microstimulator circuitry under a number of different conditions. The test results have all been very successful. This success was due to several factors, which will be discussed here along with the results that we have obtained.

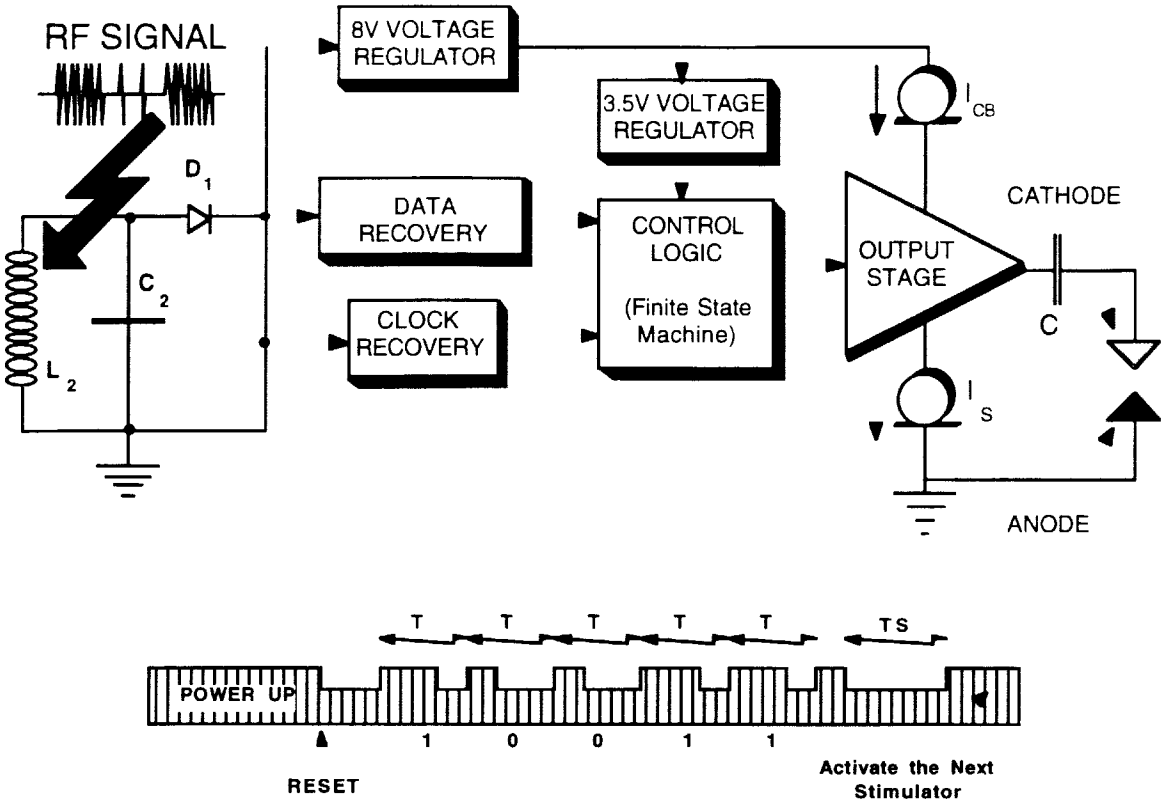

Figure 9: Overall system architecture for the first-generation microstimulator circuitry along with the data and power transmission protocol used for the RF telemetry link.

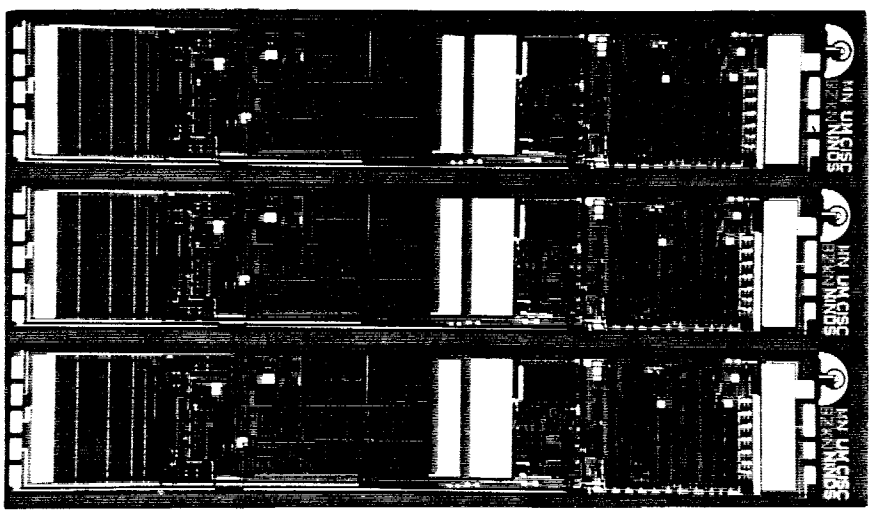

Figure 10: Photograph of the completed fabricated receiver circuitry for the single-channel microstimulator

Amplifier / Transmitter Improvements

A significant advance, both in its role in getting the microstimulator to work effectively and from a longer-term perspective of this project, was the development of an improved transmitter/amplifier design, shown in Figure 11. The basic core of the transmitter is very similar to the design discussed in depth in previous reports. The most significant difference is the addition of feedback circuitry that makes this class-E based amplifier self-oscillating. Thus, we no longer are driving the amplifier at a set frequency imposed by an external clock chip. Since the transmitter coil will be in such direct interaction with its environment and with the eventual user, it will be subject to warping and changes in behavior due to the proximity of other strong electromagnetic fields or ferromagnetic objects. These changes will consequently affect the performance of the amplifier. If the amplifier's driving frequency is fixed, then the amplifier will be driven out of its ideally tuned mode, reducing efficiency and potentially destroying amplifier components. Self-oscillation allows the amplifier to absorb such changes to a great degree within a fairly wide range of transmitter coil distortion or interaction with ferromagnetic objects. The transmitter will drift slightly in frequency, adapting to the new effective inductance caused by the alterations; however, it will remain in virtually the same mode of class-E operation. Thus, though power output may drop slightly due to frequency mismatch between the transmitter and the receiver, the amplifier will not be driven into a potentially destructive mode of operation. We have fabricated the feedback circuitry using CMOS technology and protected it in a small, integrated circuit package.

We have done some initial studies on the effectiveness of this self-oscillation technique using flexible transmitter coils of 9cm to 11cm diameter. Figure 12 illustrates the effect of coil distortion on the transmitter's frequency. Here we have defined "aspect ratio" of the coil to be the ratio of the major to minor axes. Initial results indicate a considerably linear increase in frequency as the coil is distorted. In this case, the amplifier was tuned at 2.04 MHz, the undistorted frequency. Note that for reasonable distortions, the drift in frequency is only five to ten percent. A distortion equivalent to an aspect ratio of 2.5 or more is actually very great and is hardly likely to happen under conditions of chronic use.

The proximity of large metal objects, even objects within the coil, was found to cause a slight increase in frequency (about five percent) and a decrease in the amplifier's output voltage signal of up to ten percent. However, these tests should be verified in the future, to examine the effect on an actual, working microstimulator powered telemetrically. Initial observed results with the microstimulator are encouraging.

Testing of the Microstimulator

Testing of the microstimulator essentially proceeded in three phases: testing under the probe station, without telemetry; testing under the probe station using telemetry; and telemetric testing independent of the probe station. The first phase was critical in helping us to determine what changes needed to be made in the circuitry. However, even with small nonidealities introduced intentionally in testing, the results from such probe station testing can be misleadingly good. Thus, we proceeded to test the microstimulator under the probe station, using the telemetric link. This involved overcoming several adverse effects, principally the loading introduced by numerous coaxial cables and the passive probing equipment. The results of telemetric testing under the probe station were very encouraging. Once we had determined what conditions and changes were required to operate the microstimulator telemetrically under the probe station, we proceeded to test the device telemetrically on an independent printed circuit platform, with the device wire-bonded to the board.

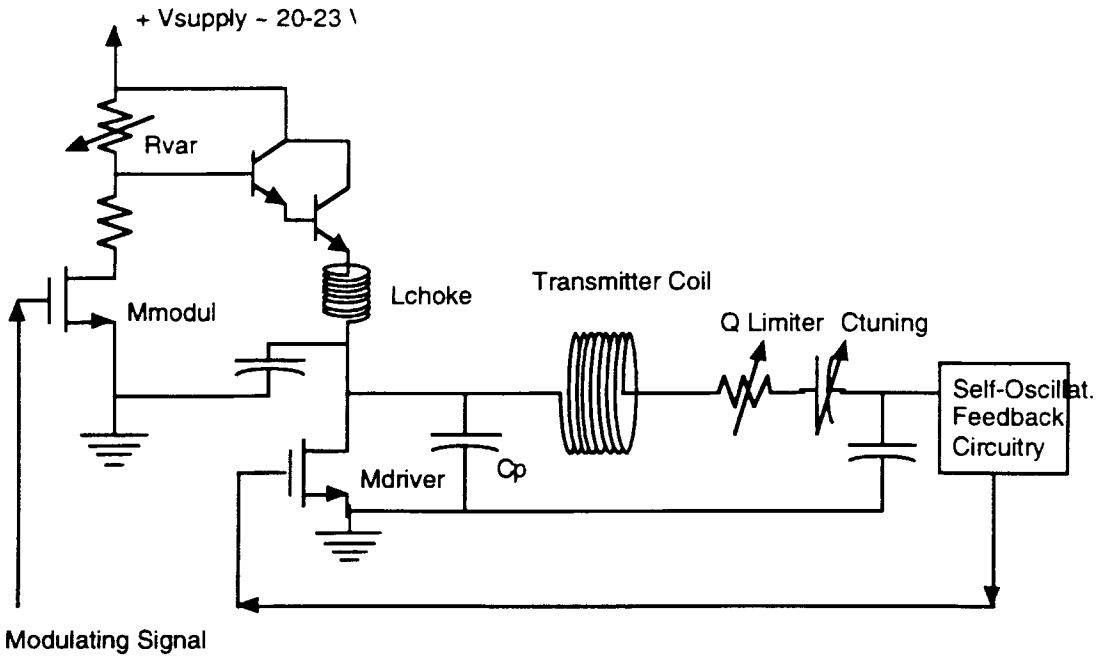

Figure 11: The overall circuit diagram of the new amplifier/transmitter.

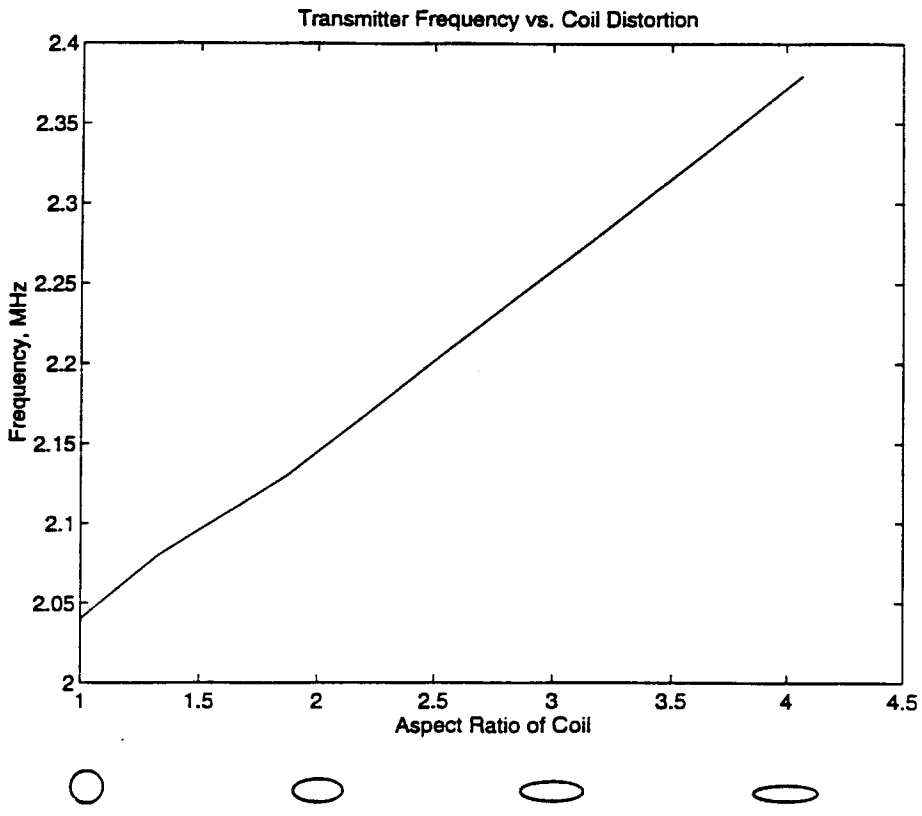

Figure 12: Transmitter frequency drift due to transmitter coil distortion is plotted here.

For this latest phase of testing, we used the basic amplifier presented previously, operating at a supply voltage of 20-23 VDC and drawing a DC average current of about 110-120mA. Thus the transmitter uses an average of 2.4 to 2.5W. Initial independent telemetric tests indicate that the microstimulator works best when its received voltage is about fifteen to twenty volts. When operating it draws about 3mA of current. The receiver portion of the microstimulator is tuned with a small (3.5mm to 3.7mm in length by 1.2mm diameter) inductor of about 45μH. The small physical size of this coil (smaller than any we have used in the past) is necessary due to size constraints of the fully packaged, glass encapsulated system. However, this leads of course to slightly weaker coupling with the transmitted signal. Thus one modification that we have had to make for now is to use a slightly smaller diameter external transmitter coil, about 6cm. Later in this section, we will discuss changes to be made to overcome this problem.

Using the described telemetric link, we obtained a fully working microstimulator. At received voltage levels of 12V or more, both voltage regulators (8V and 3.5V) work very strongly. It was found that every major subsystem of the microstimulator worked very well by telemetry. The clock signal (for a carrier frequency of about 1.9MHz) is shown in Figure 13 and can be seen to be strong and clear. The envelope detector's output (actually the negated signal from an on-chip buffer) is shown in Figure 14, along with the transmitter's output signal. The envelope detector works best when the modulation is fairly deep (about 4-5V), but its output can be seen to be very well-defined and fast. Figure 15 illustrates the output of the logic circuitry, along with the transmitter's output and the negated envelope signal. In this figure repeated pulsing is demonstrated, as the device responds to a call to leave standby mode, recognizes the address "11111" and then stimulates and returns to standby mode.

We also verified correct stimulus outputs under various conditions. If the device is not given enough time to recharge its output storage capacitor, then the output signal becomes weak and noisy, though the device continues to try to stimulate all the same. This is shown in Figure 16, in which it can be seen that the stimulus pulse is less than 2V in magnitude across a 680Ω load. This is because of the square wave signal that we have used in this case to address the device.

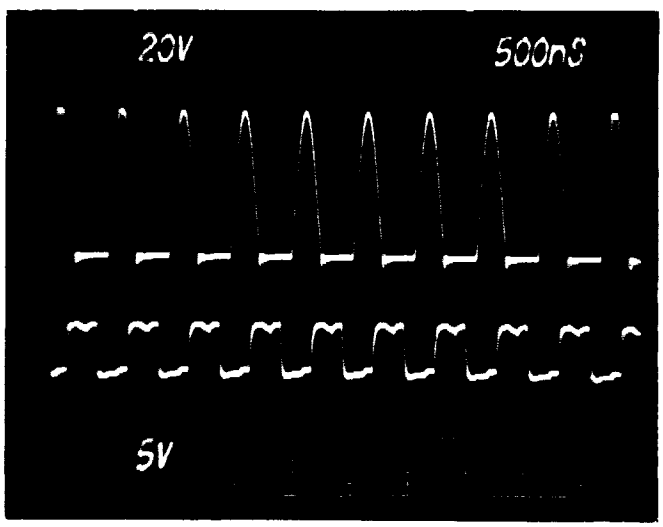

Figure 13: The microstimulator's clock output (lower trace) when operated telemetrically, along with the transmitter's output.

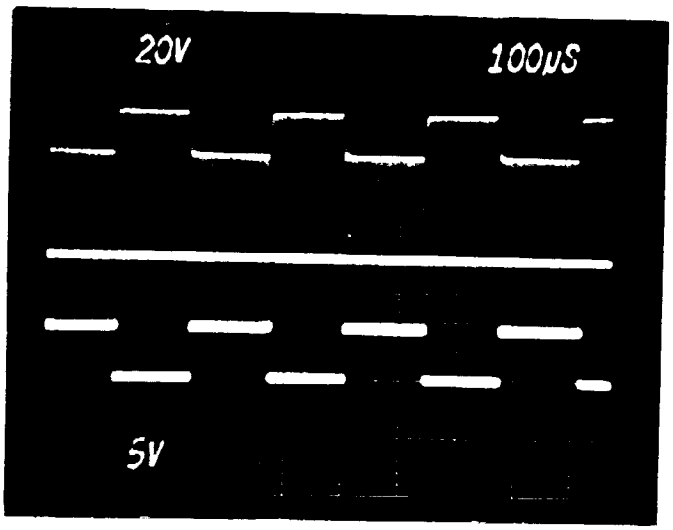

Figure 14: The buffered, negated output of the envelope detector (lower trace), along with the modulated transmitted signal.

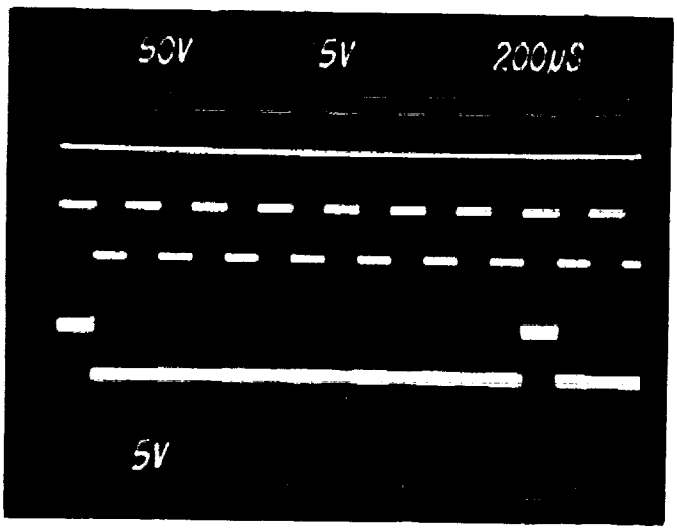

Figure 15: The logic output (lower trace, showing repetitive addressing) is seen to be strong and sharp. The upper and middle traces are the modulated transmitter output and its negated, buffered envelope from the microstimulator, respectively.

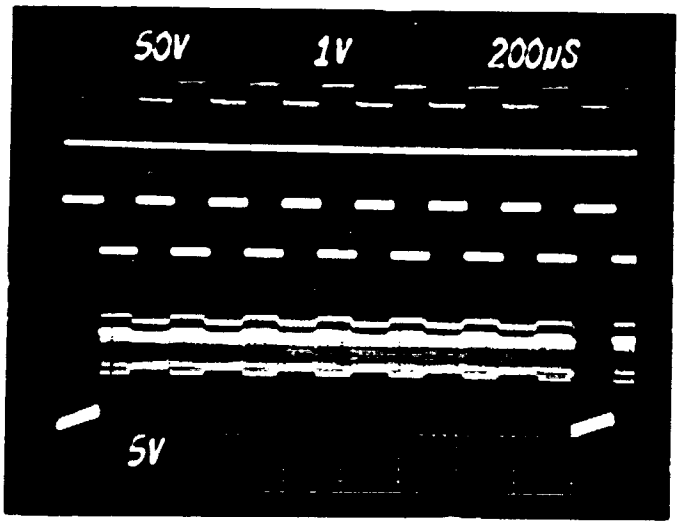

Figure 16: The effect of insufficient recharge time on the stimulus output when repeatedly addressed (lower trace) is illustrated. The middle trace is the negated microstimulator envelope of the upper trace, which is the transmitted signal.

Improvement is seen when a word generator is used, allowing us to increase the recharge time (Figure 17). However, the best results are obtained when the recharge time is at least seventy to ninety times the stimulus duration. In the case of Figures 18 and 19, the stimulus time is about 280μs and the recharge time is about 25msec. Figure 18 shows the output across a 680Ω load and 1μF storage capacitor. Also shown are the transmitter's output and the negated envelope signal. The received voltage on the chip is not shown so as not to load the receiver and alter experimental results. The carrier frequency here is close to 2MHz; the rippling effect seen on the transmitter's output signal is merely an illusion from the oscilloscope. It can be seen that the current delivered starts at about 12mA (8V/680Ω) and ends at about 9mA, averaging greater than 10mA throughout the stimulus period. The result for a 150Ω load is shown in Figure 19 under otherwise identical conditions. The stimulus pulse is flatter in the lower load case. Here the current can be seen to be slightly more than 13mA.

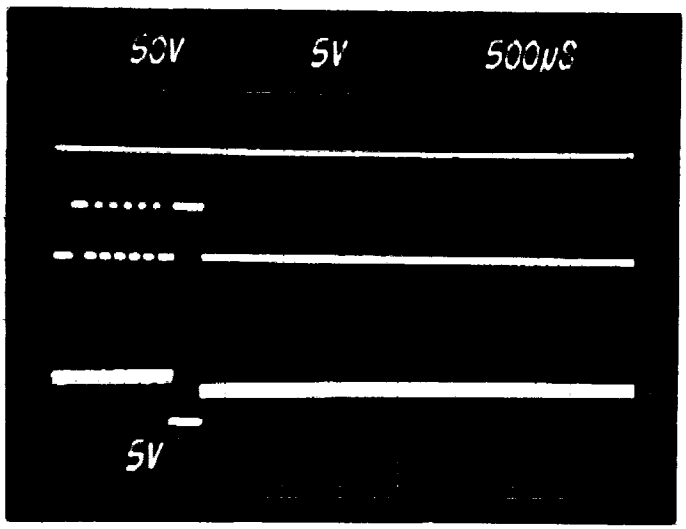

Figure 17: Given a longer recharge time between addressing, the stimulus output improves dramatically (lower trace). Again the upper and middle traces are the modulated transmitter output and its negated envelope from the microstimulator, respectively.

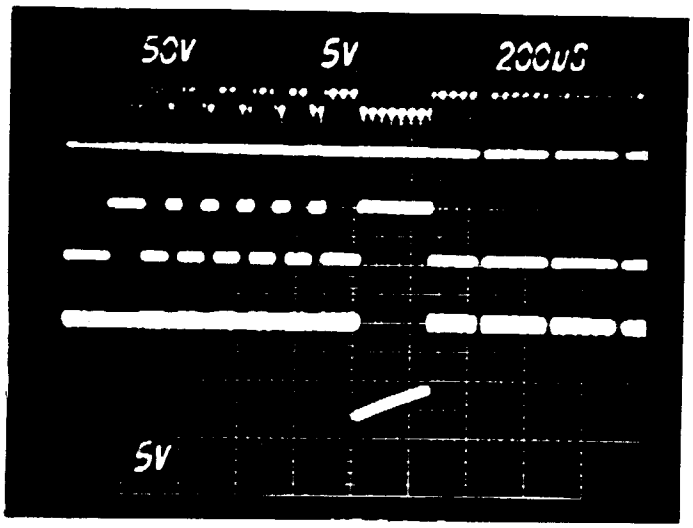

Figure 18: The lower trace illustrates the stimulus output across a 680Ω load using a 1μF storage capacitor, given the ideal minimum recharge time between stimuli. Note delivery of an average > 10mA current over 280μs. The upper trace is the modulated transmitter signal, and the middle trace is its negated envelope from the microstimulator.

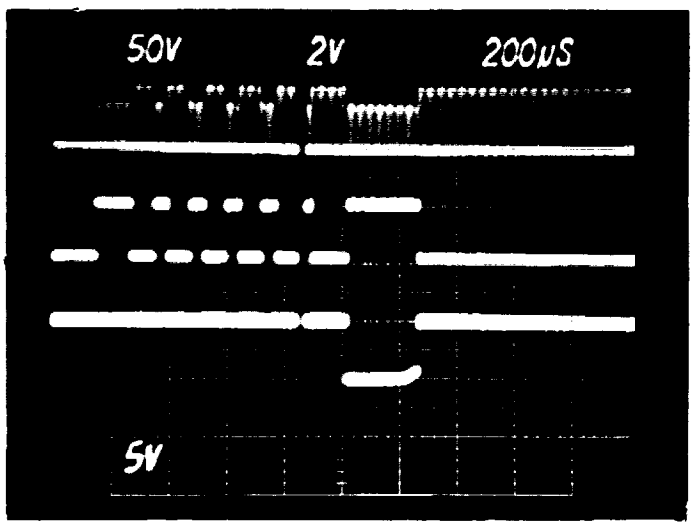

Figure 19: The lower trace now illustrates the stimulus output across a 150Ω load using a 1μF storage capacitor, given the ideal minimum recharge time between stimuli. Here an average > 13mA current is delivered over 280μs. The upper trace is the modulated transmitter signal, and the middle trace is its negated envelope from the microstimulator.

These results are very satisfactory and indicate that the circuitry is working well and can deliver sufficient current on demand. Using the above addressing pattern, we are in effect delivering currents of an average 10mA or greater for over 250μsec at about 38Hz.

Future Improvements

As mentioned previously, for these tests we used a smaller diameter transmitter coil to improve coupling. There are other ways that we may improve the performance of the link, though these involve various tradeoffs, as well. A "disadvantage," so to speak, of the self-oscillating amplifier is that the CMOS feedback responds so quickly that the amplifier is kept in near perfect class-E operation at the theoretically most efficient duty cycle of 50%. Thus the supply voltage can be increased quite a bit without drawing excessive current. The amplifier's active devices then are kept fairly free from danger of burnout. However, the amplifier's power output suffers. It would be advantageous to be able to modify the duty cycle selectively within a small range, in effect trading some efficiency for higher power output. Such modifications will be considered in the near future as an addition to the amplifier's feedback. Another way of increasing the power output for a given supply voltage is to increase the amplifier's current by using a smaller transmitter coil value. The problem is that if this involves a lower density of coil windings, then the uniformity of the transmitted field within the coil suffers. To exploit the tradeoffs involved in transmitter coil design is an art in itself, and some time will be dedicated to the production of a variety of high quality transmitter coils, including flexible ones.

Another aspect of the self-oscillating amplifier/transmitter is that it works best when tuned for high Q operation. This makes tuning between the receiver and transmitter slightly more difficult. The Q adjustment variable resistor in the design helps somewhat with this aspect. At the same time, it is very easy to fine tune the transmitter by using small variable tuning capacitors. We intend to prototype a hard-wired amplifier/transmitter on a printed circuit board soon, including space for some of these changes that we are seeing must be incorporated.

We will continue to study how best to accomplish a strong, well-tuned link now that we have the capability to test microstimulators telemetrically and independently. We will also continue to test the robustness of the microstimulator under adverse conditions, such as transmitter coil warping, proximity to metallic objects and strong electromagnetic fields, etc.

The slight changes in layout and fabrication that testing proved necessary will be incorporated soon. These should lead to dramatically improved yield and should ensure the reliability of the microstimulator circuitry.

The clock, 3.5V regulator, and control logic all work over a large input voltage range varying from less than 9V to more than 21V. The 8V regulator also operates over a large range varying from 12V to more than 21V, but will start turning off when the input voltage becomes lower than 12V. The data detection circuitry is working, however, so far it has not provided as much tolerance to input voltage variation as it was designed for. We have done many tests to determine the reason for this problem and have determined two potential sources.

We suspect that the reason for this unpredictability in the response of the envelope detector is related to the fabrication process. First, when etching the gate poly, the RIE etch recipe was not working well and the etch rate and selectivity were very low. Due to this, the etch time was more than 4 times as much as it should have been and part of the way through the etch, the photoresist masking layer was completely etched away. Toward the edge of the wafer, where the etch rate is faster, all of the polysilicon is gone. We think that the RIE etching of the gate polysilicon could be causing some of these unpredictable effects. A second problem we have identified is with the metallization step. On some dies we have noticed places where there

appears to be possible shorting between metal lines in the envelope detection circuit. This appears to be geometry dependent and occurs in the same place from die to die. Some tests that help to corroborate these explanations are the test results from the multi-channel microstimulator to be presented later.

The results of our single-channel and multi-channel microstimulator testing are very encouraging so far for obtaining a more robust single-channel device. Since our test results for the envelope detection circuitry indicate they are fabrication related, we have confidence that we will be able to have many ready circuit chips by the time we receive our new glass capsule packages next month. With some minor process modifications we should have no problem obtaining an envelope detector that can operate over as large of an input voltage range as the rest of the circuitry. The changes involve modification only to the metal interconnect layer of the circuitry and do not require complete refabrication. As was stated in the beginning of this section, we have many wafers at various points in processing and can produce more devices in as little time as 2 days, and the wafers that are farther behind in the process can be finished in 3 weeks.

2.2.2 Multi-Channel Microstimulator

Figure 20 shows a system block diagram of the multi-channel microstimulator. This device was on the same mask set and fabrication process as the single-channel device discussed above. Figure 21 shows a photograph of the fabricated multi-channel microstimulator with the various circuit blocks labeled. We have been able to test the clock, voltage regulators, envelope detector, and on-chip transmitter so far. All of these circuits have produced very good results. Figure 22 shows an output trace of the 9V and 4.5V regulators for a 1.8MHz sinusoidal input with a peak of 19V. These voltage supplies provide very good regulation over a wide input voltage range from 12V to 21V and consume less than one fifth the power of the single-channel regulator design. The clock design is the same as was used for the single-channel device and also had no problems functioning over a wide input voltage range.

The envelope detector for the multi-channel device is the same design as was tested in the single-channel device. The initial testing shows that this circuit is working very close to what we expected. The testing we have done so far has worked very well even without any modification of the programmable links. This circuit has worked well in testing with an input voltage range varying from 10V to 21V and an envelope modulation depth ranging from 2V to more than 6V. The layout of this circuit is almost exactly the same as that on the single-channel design. An explanation for the difference in results from testing the two designs is that the multi-channel design is closer to the center of the wafer and would not be affected as much by the RIE polysilicon etch. There are also some slight differences in the routing of interconnect metal lines, and we have not noticed the same metallization problems with this design, possibly due to the slightly different interconnect geometry.

The on-chip transmitter has been tested so far by bonding it to a 1μH micromachined coil. The fabrication process for these coils has been discussed in previous reports. Figure 23 shows the voltage across a coil connected to an operating transmitter. The transmitter coil voltage is ≈2.5V peak-to-peak, and the average current consumption is 1.2mA. The transmission frequency is 33MHz. In our initial testing, we have been able to receive this transmitted signal several feet away with an unbuffered and unfiltered receiver coil. Figure 24 shows the output signal from a coil whose received voltage is being fed directly input an oscilloscope. The trace shows the received signal as the transmitter is being modulated on and off. The received voltage has a peak amplitude of ≈5mV and has a rise and fall time of ≤500ns. This signal is very detectable, and with proper filtering and signal buffering, we should easily be able to detect this transmitted signal even in the presence of the large external transmitter signal.

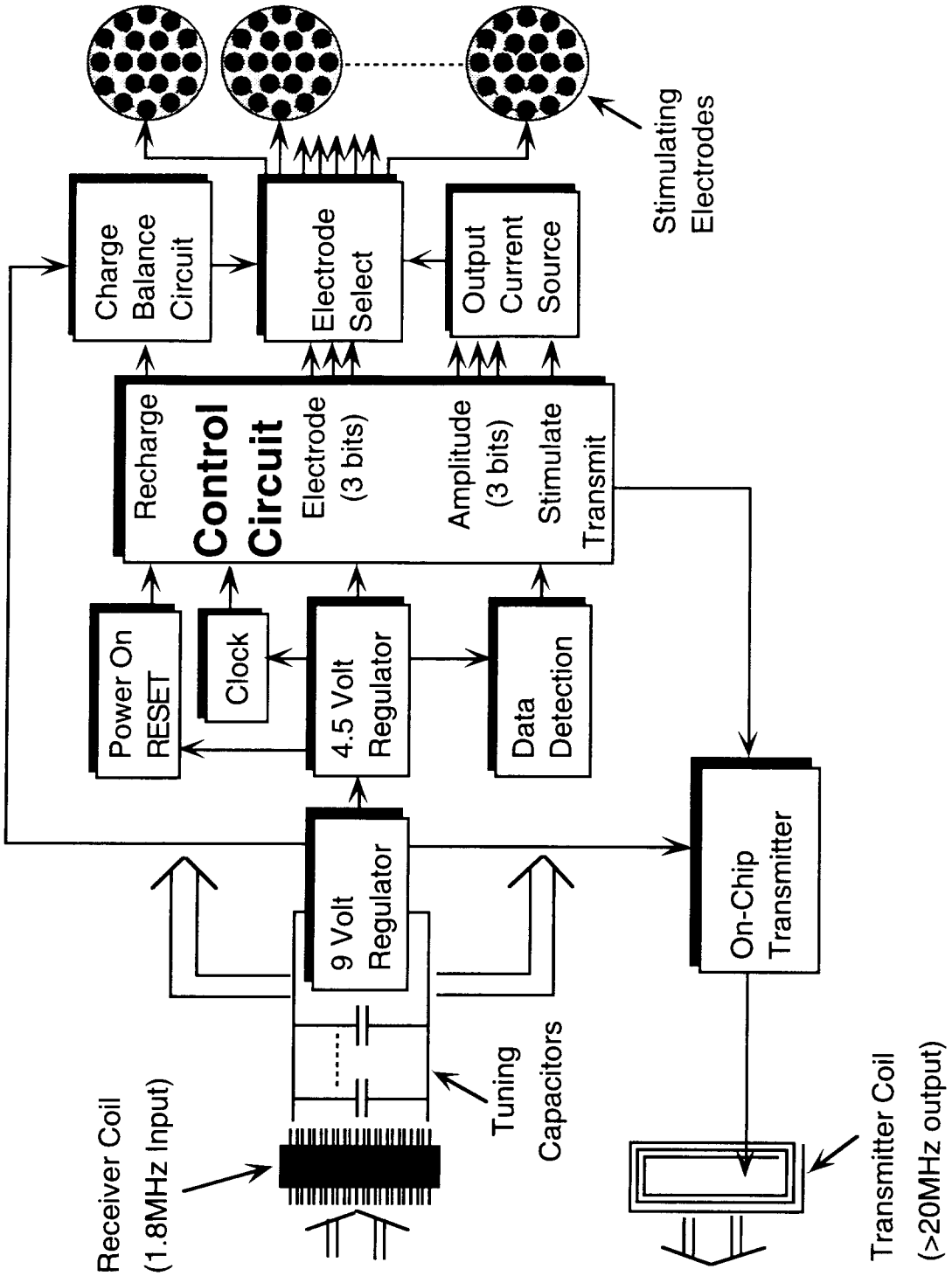

Figure 20: Block diagram of a fault-tolerant multi-channel microstimulator system with bidirectional telemetry

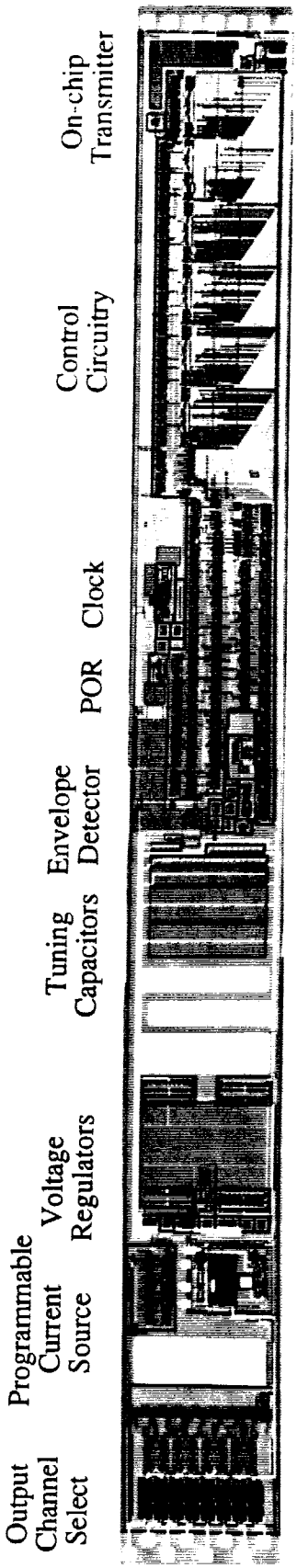

Figure 21: Photograph of the fabricated multi-channel microstimulator circuitry.

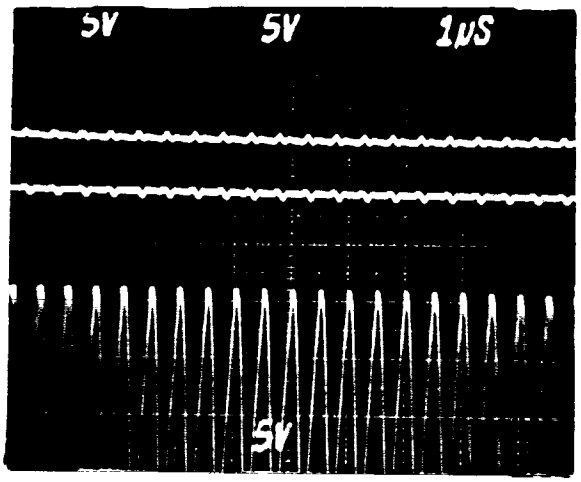

Figure 22: Output of 9V and 4.5V regulators with a 20Vpeak 1.8MHz sinusoidal input voltage.

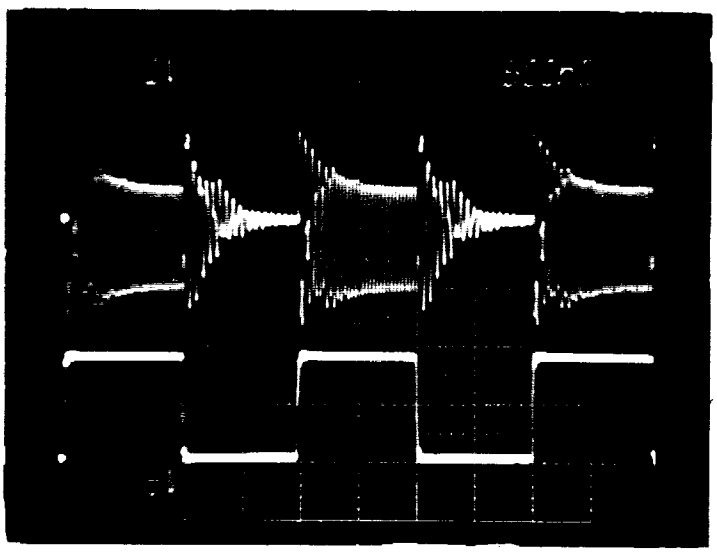

Figure 23: Voltage across a 1μH transmitter coil for an on-chip transmitter operating at 33MHz and consuming 1.2mA.

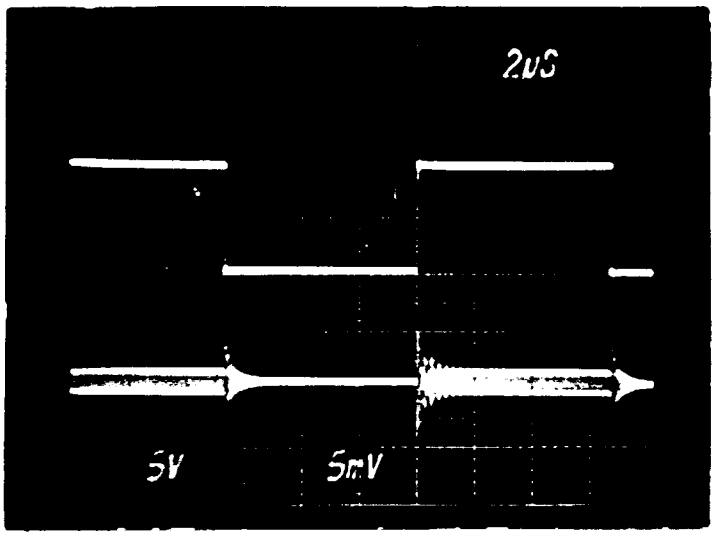

Figure 24: Voltage received across an unbuffered and unfiltered receiver coil at >2 feet distance from an on-chip transmitter.

The testing of the multi-channel microstimulator has just started and additional results will be provided in the next progress report. The early results are very encouraging and important. In particular, the results obtained from the on-chip transmitter are very important not only for this device but also for future long-term testing of the packages. As was specified in our statement of work, we are supposed to develop systems for remote testing of the hermeticity of our packages. This will require a telemetry link to transmit information on the integrity of the package to the outside world. We believe that the on-chip transmitters will be an important part of this remote testing block, and we intend to use these transmitters in future testing of our packages both in-vitro and in-vivo.

3. Plans for the Coming Quarter:

Our activities for the coming quarter will proceed in several areas. First, we will focus most of our efforts on continuing our package tests and on the fabrication of the new substrates and glass capsules. As was mentioned before, we should receive the first batch of ultrasonically-machined glass capsules soon. These capsules will be diced apart and subjected to accelerated soak tests as soon as the silicon substrates are ready. A new mask set has been finished for the silicon substrates and will be used to fabricate the necessary devices for testing the new packages. The tests will involve temperature accelerated tests similar to those currently under way. These tests will be complemented by additional tests to determine the failure modes and to isolate various leakage paths into the package. We will discuss our approach in this regard in future reports. In addition to in-vitro tests, we will continue to increase our testing under in-vivo conditions. Initial in-vivo tests have already been started at Michigan and these will soon be complemented by tests to be performed at Vanderbilt. We will fabricate in-vivo packages with on-chip humidity and dew-point sensors so that we can tests for hermeticity in-situ.

We will also continue our testing and assembly of complete microstimulators. Now that the first-generation microstimulators have been completed we hope to provide these devices to users who can implant them in various animal models. We plan on having a number of these devices ready for testing by external users. The multi-channel microstimulators will be fully tested and if test results continue to be encouraging we will proceed with the development of complete systems for in-vivo use. We anticipate that these second-generation devices will be completely tested and available by the end of summer.